doi:10.1093/brain/awx040 BRAIN 2017: 140; 1267–1279 | 1267

BRAIN
A JOURNAL OF NEUROLOGY

ZNHIT3 is defective in PEHO syndrome, a severe encephalopathy with cerebellar granule neuron loss

Anna-Kaisa Anttonen,[1,2,3,4,*] Anni Laari,[1,2,3,*] Maria Kousi,[5,*] Yawei J. Yang,[6] Tiina Jääskeläinen,[7,8] Mirja Somer,[9] Eija Siintola,[1,2] Eveliina Jakkula,[10] Mikko Muona,[1,2,3,10] Saara Tegelberg,[1,2,3] Tuula Lönnqvist,[11] Helena Pihko,[11] Leena Valanne,[12] Anders Paetau,[13] Melody P. Lun,[14,15] Johanna Hästbacka,[1,16,†] Outi Kopra,[1,2,3,#] Tarja Joensuu,[1,2,3] Nicholas Katsanis,[5] Maria K. Lehtinen,[14] Jorma J. Palvimo[7] and Anna-Elina Lehesjoki[1,2,3]

[*]These authors contributed equally to this work.
[#]Deceased.

Progressive encephalopathy with oedema, hypsarrhythmia, and optic atrophy (PEHO) syndrome is an early childhood onset, severe autosomal recessive encephalopathy characterized by extreme cerebellar atrophy due to almost total granule neuron loss. By combining homozygosity mapping in Finnish families with Sanger sequencing of positional candidate genes and with exome sequencing a homozygous missense substitution of leucine for serine at codon 31 in *ZNHIT3* was identified as the primary cause of PEHO syndrome. *ZNHIT3* encodes a nuclear zinc finger protein previously implicated in transcriptional regulation and in small nucleolar ribonucleoprotein particle assembly and thus possibly to pre-ribosomal RNA processing. The identified mutation affects a highly conserved amino acid residue in the zinc finger domain of ZNHIT3. Both knockdown and genome editing of *znhit3* in zebrafish embryos recapitulate the patients' cerebellar defects, microcephaly and oedema. These phenotypes are rescued by wild-type, but not mutant human *ZNHIT3* mRNA, suggesting that the patient missense substitution causes disease through a loss-of-function mechanism. Transfection of cell lines with ZNHIT3 expression vectors showed that the PEHO syndrome mutant protein is unstable. Immunohistochemical analysis of mouse cerebellar tissue demonstrated ZNHIT3 to be expressed in proliferating granule cell precursors, in proliferating and post-mitotic granule cells, and in Purkinje cells. Knockdown of *Znhit3* in cultured mouse granule neurons and *ex vivo* cerebellar slices indicate that ZNHIT3 is indispensable for granule neuron survival and migration, consistent with the zebrafish findings and patient neuropathology. These results suggest that loss-of-function of a nuclear regulator protein underlies PEHO syndrome and imply that establishment of its spatiotemporal interaction targets will be the basis for developing therapeutic approaches and for improved understanding of cerebellar development.

1 The Folkhälsan Institute of Genetics, Haartmaninkatu 8, 00290 Helsinki, Finland
2 Neuroscience Center, University of Helsinki, Viikinkaari 4, 00790 Helsinki, Finland
3 Research Programs Unit, Molecular Neurology, University of Helsinki, Haartmaninkatu 8, 00290 Helsinki, Finland
4 Medical and Clinical Genetics, University of Helsinki and Helsinki University Hospital, Haartmaninkatu 8, 00290 Helsinki, Finland
5 Center for Human Disease Modeling, Duke University Medical Center, Carmichael Building, 300 North Duke Street, Suite 48-118, Durham, NC 27701, USA
6 Division of Genetics, Howard Hughes Medical Institute, and Manton Center for Orphan Disease Research, Children's Hospital Boston, Program in Biological and Biomedical Sciences, Harvard Medical School, and Harvard-MIT Division of Health Sciences and Technology, Harvard Medical School, BCH 3150, 300 Longwood Ave., Boston, MA 02115, USA
7 Institute of Biomedicine, University of Eastern Finland, Yliopistonranta 1, 70210 Kuopio, Finland

Received September 18, 2016. Revised December 18, 2016. Accepted January 6, 2017. Advance Access publication March 1, 2017.

8 Institute of Dentistry, University of Eastern Finland, Yliopistonranta 1, 70210 Kuopio, Finland
9 The Norio Centre, The Rinnekoti Foundation, Kornetintie 8, 00380 Helsinki, Finland
10 Institute for Molecular Medicine Finland, University of Helsinki, Haartmaninkatu 8, 00290 Helsinki, Finland
11 Department of Pediatric Neurology, Children's Hospital, University of Helsinki and Helsinki University Hospital, Lastenlinnantie 2, 00290 Helsinki, Finland
12 Department of Radiology, HUS Medical Imaging Center, Haartmaninkatu 4, 00290 Helsinki, Finland
13 Department of Pathology, Helsinki University Hospital, Haartmaninkatu 3, 00290 Helsinki, Finland
14 Department of Pathology, Boston Children's Hospital, BCH 3108, 300 Longwood Ave., Boston, MA 02115, USA
15 Department of Pathology and Laboratory Medicine, Boston University School of Medicine, 670 Albany Street, Boston, MA 02118, USA
16 Department of Pediatrics, Children's Hospital, University of Helsinki and Helsinki University Hospital, Stenbäckinkatu 11, 00290 Helsinki, Finland

†Present address: Department of Perioperative, Intensive Care and Pain Medicine, University of Helsinki and Helsinki University Hospital, Stenbäckinkatu 11, 00290 Helsinki, Finland

Correspondence to: Anna-Elina Lehesjoki,
The Folkhälsan Institute of Genetics, Haartmaninkatu 8,
00290 Helsinki,
Finland
E-mail: anna-elina.lehesjoki@helsinki.fi

Keywords: PEHO syndrome; progressive encephalopathy; ZNHIT3; cerebellum

Abbreviations: CRISPR = clustered regularly-interspaced short palindromic repeats; dpf = days post-fertilization; GFP = green fluorescent protein; MO = morpholino oligonucleotide; PEHO = progressive encephalopathy with oedema, hypsarrhythmia, and optic atrophy

Introduction

PEHO syndrome (progressive encephalopathy with oedema, hypsarrhythmia, and optic atrophy; MIM 260565) is a rare disorder with distinctive neuroradiological and neuropathological findings. The diagnostic criteria include infantile-onset hypotonia, infantile spasms with hypsarrhythmia, profound psychomotor retardation, optic atrophy, and progressive brain atrophy primarily involving the cerebellum and brainstem (Somer, 1993*a*; Somer *et al.*, 1993*a*). Additional clinical findings include typical facial dysmorphism (Fig. 1A), oedema of the face and limbs (Fig. 1B), brisk tendon reflexes in early childhood, abnormal brainstem auditory evoked potentials, slowed nerve conduction velocity in late childhood, and dysmyelination observed on MRI (Fig. 1C–G) (Salonen *et al.*, 1991; Somer, 1993*a*; Somer and Sainio, 1993; Somer *et al.*, 1993*a*,*b*). Head circumference is average at birth, but drops to −2 standard deviations during infancy (Somer, 1993*a*). Microcephaly at birth, abnormal gyral formation, predominant spasticity in infancy, reappearance of visual contact after cessation of infantile spasms, hepato- or splenomegaly and storage disorder in histological studies argue against diagnosis of PEHO syndrome (Somer, 1993*a*). There is cerebral and extreme cerebellar cortical atrophy (Fig. 1H), with the inner granule cell layer being either totally absent or containing only few neurons and the Purkinje cells showing abnormal dendritic arborization and misalignment (Haltia and Somer, 1993). The optic nerves show loss of myelinated axons and gliosis, while the retinal nerve fibre and ganglion cell layers are atrophic (Somer *et al.*, 1993*b*).

PEHO syndrome is enriched in the Finnish population with an estimated incidence of 1:74 000 (Somer, 1993*a*) and ∼30 clinically diagnosed patients. PEHO syndrome is very rare in other populations with <25 reported patients (Field *et al.*, 2003; Alfadhel *et al.*, 2011; Caraballo *et al.*, 2011). Patients with PEHO-like features are more common and present with many but not all characteristic findings of PEHO syndrome, e.g. have atypical neuroradiological findings or show no sign of progression (Chitty *et al.*, 1996; Field *et al.*, 2003; Longman *et al.*, 2003). Recessive disease-causing variants in the *SEPSECS* gene involved in selenoprotein biosynthesis have been described in four Finnish patients with PEHO-like features (Anttonen *et al.*, 2015), but the cause for autosomal recessive PEHO syndrome has remained unknown.

Here we report the identification of a missense loss-of-function variant in *ZNHIT3* as the primary defect underlying PEHO syndrome. Using knockdown and genome editing experiments in zebrafish embryos and knockdown experiments in mouse cerebellar neurons, we show that ZNHIT3 is essential for normal cerebellar development.

Materials and methods

Study subjects

The study included 23 Finnish patients with a clinical diagnosis of PEHO and 40 Finnish and 47 non-Finnish patients with

PEHO-like features. In addition, clinical information was available from three patients with a clinical diagnosis of PEHO but DNA sample available only from parents. The study was approved by an Institutional Review Board at the Helsinki University Hospital and written informed consent was obtained from all study subjects or their legal guardians according to the Declaration of Helsinki prior to drawing peripheral blood for DNA extraction.

Homozygosity mapping and sequencing

DNA samples of 11 patients were genotyped using the Illumina HumanHap300-duo single nucleotide polymorphism (SNP) microarrays (Illumina) containing over 318 000 SNPs. Illumina Beadstudio v3.1.0 was used to call genotypes and all samples had >99% call rate. Plink version 1.02 (Purcell *et al.*, 2007) was used to search for extended tracts of homozygosity in each sample using a minimum length of 50 SNPs and 400 kb. The coding regions of the six positional candidate genes (Supplementary Table 1) were Sanger sequenced from genomic DNA using three patient samples (Patients a3, d3, and n4; Supplementary Fig. 1). Primers are available upon request. One patient (Patient a5; Supplementary Fig. 1) was whole-exome sequenced. The sequencing protocol and sequence data analysis are described in the Supplementary material.

Morpholino knockdown in zebrafish embryos

The experimental work was carried out under protocols approved by the Institutional Animal Care and Use Committee, Duke University, following standard laboratory procedures in accordance with the Duke Animal Care and Use Program. We injected 1 nl (15 ng) of the translation-blocking morpholino oligonucleotide (MO), *znhit3*_MO, into wild-type zebrafish embryos at the 1–2-cell stage and for the rescue experiments 100 pg of relevant human mRNA. To evaluate CNS integrity and oedema, injected embryos were raised until 3 days post-fertilization (dpf); they were scored for cardiac and/or generalized oedema and subsequently processed for CNS analysis through whole-mount staining using an antibody against acetylated tubulin (T7451, Sigma-Aldrich). To evaluate differentiated granule cell expression in the cerebellum of 5 dpf developing zebrafish larvae, we injected a NeuroD:GFP reporter line (Drerup and Nechiporuk, 2013). For more detailed methods, see Supplementary material.

Generation of CRISPR mutant zebrafish embryos

For the CRISPR (clustered regularly-interspaced short palindromic repeats) experiments, *znhit3* guide RNA was generated as described (Jao *et al.*, 2013). The protocols for generation of *znhit3* guide RNA and F0 CRISPR mutant zebrafish are described in the Supplementary material. To generate the F1' compound heterozygous or homozygous mutant *znhit3* embryos we intercrossed F0 adult founders. From each of the produced clutches eight embryos were sacrificed, subjected to T7 endonuclease I assay and Sanger sequenced to determine the exact genotype and zygosity. Matings from two pairs yielded 100% of the eight embryos tested with recessive events and were subsequently phenotyped to assay the integrity of the cerebellum as well as the head size (Fig. 3). The MO and CRISPR phenotypic outcomes were qualitatively and quantitatively concordant in their impact on cerebellar integrity by counting the embryos with cerebellar abnormalities as visualized by acetylated tubulin staining and measuring of the area covered by NeuroD:GFP$^+$ cells, respectively.

Expression plasmids and site-directed mutagenesis

The cDNA clone of human *ZNHIT3* was purchased from imaGenes and cloned into pcDNA3.1 vector (Invitrogen) and into the haemagglutinin (HA) tag containing pAHC expression vector, a derivative of the pCIneo expression vector (Promega). The c.92C>T nucleotide change was introduced into the wild-type construct using the QuickChange Lightning Site-Directed Mutagenesis Kit (Stratagene) and verified by sequencing.

Cell culture experiments, immunoblotting and immunocytochemistry

For measurement of protein stability, HeLa, COS-1 and BHK cells (from ATCC) were cultured, transfected and exposed to protein synthesis inhibitor cycloheximide or proteasome inhibitor MG132 and analysed by immunoblotting as described in detail in the Supplementary material. Cerebellar granule cell cultures were prepared from postnatal Day 5 mice (C57BL) and cultured for 2 days *in vitro*, as described previously (Giulian and Baker, 1986; Lehtinen *et al.*, 2009). HeLa, BHK and mouse cerebellar granule cells were processed for immunocytochemical confocal imaging analyses using Zeiss LSM 700 or 780 microscope as described in detail in the Supplementary material. Primary antibodies used were a rabbit antibody to human ZNHIT3 (A301-214A, Bethyl Laboratories; 1:200), a goat antibody to human lamin B1 (Santa Cruz Biotechnology; 1:1000) and a mouse antibody to tubulin, beta III isoform (Chemicon; 1:200). Image processing was done with ImageJ and Adobe Photoshop CS4 software.

Immunohistochemistry

Immunohistochemistry was done on sagittal paraffin sections of embryonic Day 16.5, postnatal Day 3, and postnatal Day 10 or 21 mouse brain (see Supplementary material for details). Primary antibodies used were a rabbit antibody to ZNHIT3 (A301-231A; Bethyl Laboratories, 1:600), a mouse antibody to CDC47 (Thermo Scientific; 1:100), a mouse antibody to glial fibrillary acidic protein (GFAP) (M076101-2, Dako, Agilent Technologies, 1:150) and a mouse antibody to calbindin (Swant, 1:1000). The slides were analysed with Zeiss Axioplan 2 epifluorescence (Fig. 5A) or with Zeiss LSM 780 Confocal microscope (Fig. 5B) and with AxioVision 3.1 or Zen 2010 software, respectively. Image processing was done with ImageJ and Adobe Photoshop software.

RNAi plasmid design

Mammalian hairpin (hp) RNA interference (RNAi) constructs were designed as described (Gaudilliere *et al.*, 2002). The hpRNA targeting sequences are: GAAGAAGACAGAGT GTCTCTG (*Znhit3*) and TACGCGCATAAGATTAGGGTA (Scramble) (Christensen *et al.*, 2011). *Znhit3* rescue was generated by creating five silent base-pair mutations into the wild-type cDNA encoding ZNHIT3 using the QuikChange Site-Directed Mutagenesis Kit (Stratagene) as follows: GAGGAT AGAGTCTCGCTC.

Survival assay

Cerebellar granule neurons prepared from postnatal Day 5 mouse cerebella were transfected with the hpRNA constructs as described (Lehtinen *et al.*, 2006). Briefly, cultures were transfected at postnatal Day 5 + 2 days *in vitro* (DIV) by the calcium phosphate method. Seventy-two hours later, cells were subjected to immunocytochemistry using an antibody to green fluorescent protein (GFP) (Abcam), and neuronal survival was assessed in a blinded manner in transfected GFP-positive neurons based on the integrity of neuronal processes and nuclear morphology (Hoechst) (Lehtinen *et al.*, 2006).

Cerebellar slice cultures

Cerebella were harvested from postnatal Day 8 C57/Bl6 mouse pups, immersed in plasmid DNA (2 μg/μl) in complete Hanks Balanced Salt Solution (HBSS), transferred to a CUY520-P5 Platinum block Petridish Electrode (Protech International), and electroporated with an ECM 830 square wave electroporator (BTX Genetronics) at 80 V, five pulses, 50 ms pulse, and 500 ms interval. Electroporated cerebella were embedded in 3% low melting point agarose in HBSS, and 250 μm coronal or sagittal cerebellar slices were prepared using a VT1000S Vibratome (Leica Microsystems). Slices were transferred to Millicell® tissue culture inserts (Millipore) and cultured in Eagle's Basal Medium, with 1 mM L-glutamine, 0.5% glucose, and ITS (Sigma) and 50 U/ml penicillin and streptomycin and analysed at 48 or 72 h post-plating. The location of GFP-positive staining cerebellar granule neurons was quantified with respect to location of the Purkinje cell layer and interpreted as migration as described (Yang *et al.*, 2012). Slices were imaged using BioGBS Zeiss 510 and analysed using ImageJ and Amaxa softwares.

Statistical analyses

Zebrafish embryos were analysed in a blinded manner. The Pearson χ^2 test was used for cerebellar integrity and oedema assays. In evaluating the area of the optic tectum and the area covered by granule cells in NeuroD:GFP larvae, differences of means by condition was calculated using a two-tailed Student's *t*-test. Statistical significance was determined when $P < 0.05$.

For cerebellar granule cell survival ~150 cells were counted per treatment condition, per experiment, in a blinded manner and analysed for statistical significance by ANOVA followed by Fisher's Protected Least Significant Difference *post hoc* test. Statistical analyses represent a minimum of three separate experiments with $P < 0.05$ considered as significant. The location of GFP-positive cerebellar granule neurons was analysed in a double-blind manner and quantified using unpaired *t*-test.

Results

Identification of the *ZNHIT3* gene underlying PEHO syndrome

Homozygosity mapping in 11 Finnish patients with PEHO syndrome (Supplementary Fig. 1) defined a 433-kb region on chromosome 17q12 (data not shown); none of 427 genotyped Finnish control individuals were homozygous. Sanger sequencing of coding regions of the six positional candidate genes in three patients (Patients a3, d3, and n3; Supplementary Fig. 1) revealed a homozygous rare missense variant, c.92C > T (p.Ser31Leu), in *ZNHIT3* (MIM 604500; NM_004773.3), which encodes the zinc finger HIT domain-containing protein 3 (ZNHIT3). Other genes were excluded based on high population frequencies of the identified variants (Supplementary Table 1). Whole-exome sequencing in one patient with PEHO (Patient a5; Supplementary material) identified the c.92C > T variant as the only homozygous protein coding variant in the six positional candidate genes (Supplementary Table 1).

Of the remaining 19 Finnish patients with clinically diagnosed PEHO syndrome, 18 were homozygous for c.92C > T. The one patient with no mutations in *ZNHIT3* had progressive cerebellar atrophy, determined by CT, and hypoplastic (as opposed to atrophic) optic discs. Two of 40 Finnish patients with PEHO-like features were homozygous for c.92C > T. One of these patients lacked a history of infantile spasms and hypsarrhythmia, though he otherwise fulfilled the clinical criteria. The second patient initially had neuroimaging findings atypical for PEHO syndrome, but these were later attributed to use of vigabatrin, an anti-epileptic drug that inhibits breakdown of GABA (Walker and Kälviäinen, 2011). None of the 47 non-Finnish PEHO-like patients had mutations in *ZNHIT3*.

The c.92C > T variant segregated in an autosomal recessive manner in affected families. The carrier frequency in the entire Exome Aggregation Consortium database was 0.07% (40/58 895 individuals) and 0.92% (31/3350) among Finnish individuals, with no homozygous individuals detected. The 155-amino acid ZNHIT3 polypeptide (NP_004764.1) contains a N-terminal (amino acids 11–42) cysteine-rich histidine triad motif -type zinc finger (zf-HIT) domain (Fig. 2) found in nuclear proteins implicated in transcription regulation and chromatin remodelling (Iwahashi *et al.*, 2002; He *et al.*, 2007; Cuadrado *et al.*, 2010). It also contains a conserved LxxLL motif (Fig. 2A) present in many nuclear receptor coregulators (Heery *et al.*, 1997). The p.Ser31Leu substitution affects a highly conserved residue of the zf-HIT domain located next to one of the zinc-coordinating cysteines (Fig. 2B), and based on

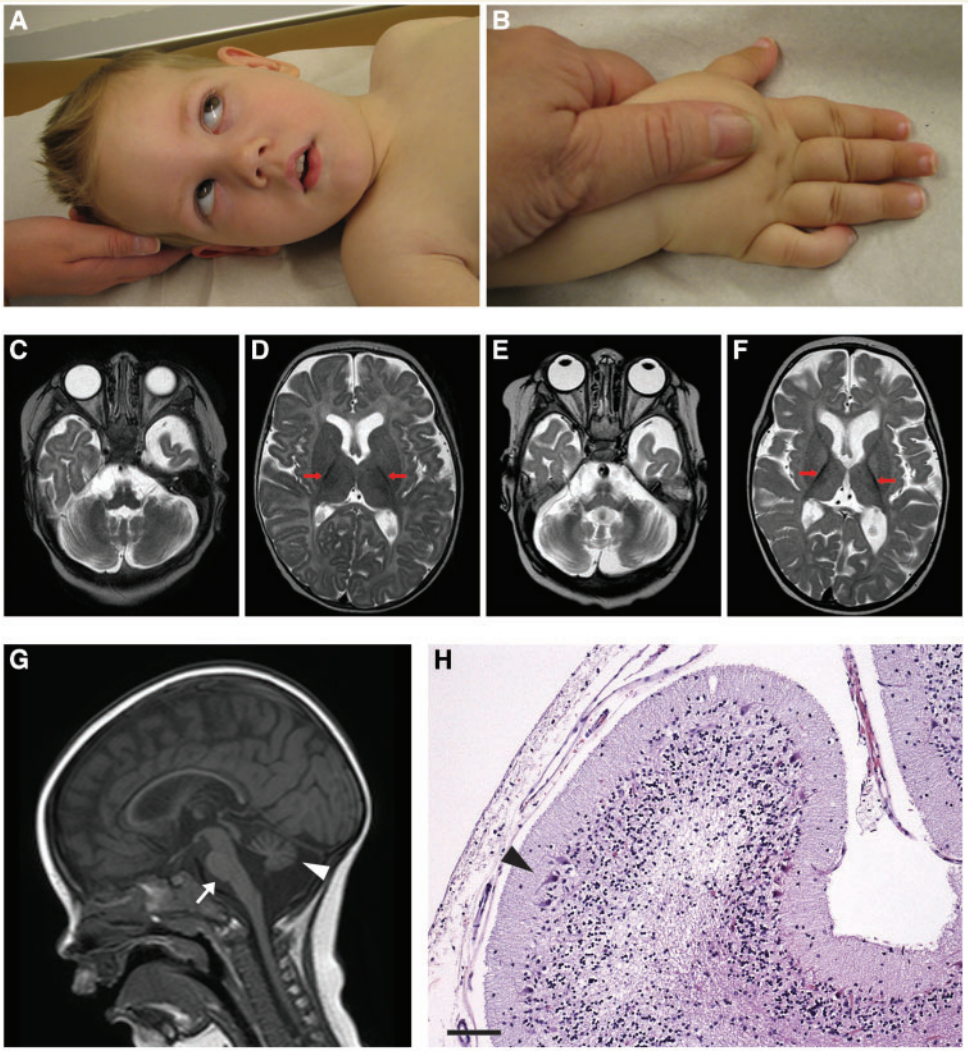

Figure 1 Phenotypic features of PEHO syndrome. (**A**) Facial features of a patient at 1 year 2 months. Note the narrow forehead, epicanthic folds, outward turning ear lobules, and open mouth. (**B**) The hands show oedema and the fingers are tapering. (**C**) Axial MRI at the age of 5 months shows marked cerebellar atrophy. The supratentorial CSF spaces are normal. (**D**) At 5 months the myelination is almost normal for the age (arrows). (**E**) At 1 year of age, cerebellar atrophy has progressed and is now severe and (**F**) myelination has proceeded only slightly and is now markedly abnormal for the age (arrows). (**G**) In midline sagittal MRI at 1 year of age pons (arrowhead) is also atrophic, but not to the same degree as the cerebellum (arrow). The supratentorial brain shows atrophy. (**H**) Atrophic cerebellar cortex from a PEHO patient (3 years 4 months). Haematoxylin and eosin-stained paraffin section showing an atrophic folium with clearly thinned molecular layer, almost total loss of Purkinje cells, and prominent atrophy of the granule cell layer. The remaining Purkinje cells are pyknotic and disaligned (arrowhead). Original magnification × 100; Scale bar = 100 μm. Consent to publish facial images of the subject was obtained.

three of four *in silico* predictions (Supplementary Table 1), is deleterious. Collectively, these genetic data strongly suggest that c.92C > T is the mutation causing PEHO syndrome.

Knockdown and genome editing of *znhit3* in zebrafish

To get further biological causal evidence and to establish the direction of effect of the p.Ser31Leu substitution, we developed *in vivo* surrogate zebrafish models. A BLASTp query of the zebrafish protein against the human proteome identified the human ZNHIT3 as the major hit. RNA *in situ* hybridization of the single *znhit3* orthologue (66% similarity; 49% identity) showed widespread expression across the head of 5 dpf larvae (Supplementary Fig. 2). Suppression of *znhit3* by antisense morpholino injection induced dosage-sensitive defects in a number of organs relevant to human pathology. These included microcephaly (through the surrogate measurement of the area of the optic tectum) (Schulte *et al.*, 2014; Borck *et al.*, 2015) and structural cerebellar defects (Fig. 3) as well as pericardiac oedema (Supplementary Fig. 3). These phenotypes were specific. First, we were able to rescue all the above pathologies by co-injecting embryos with wild-type human *ZNHIT3* capped mRNA ($P = 0.002$ for the optic tectum

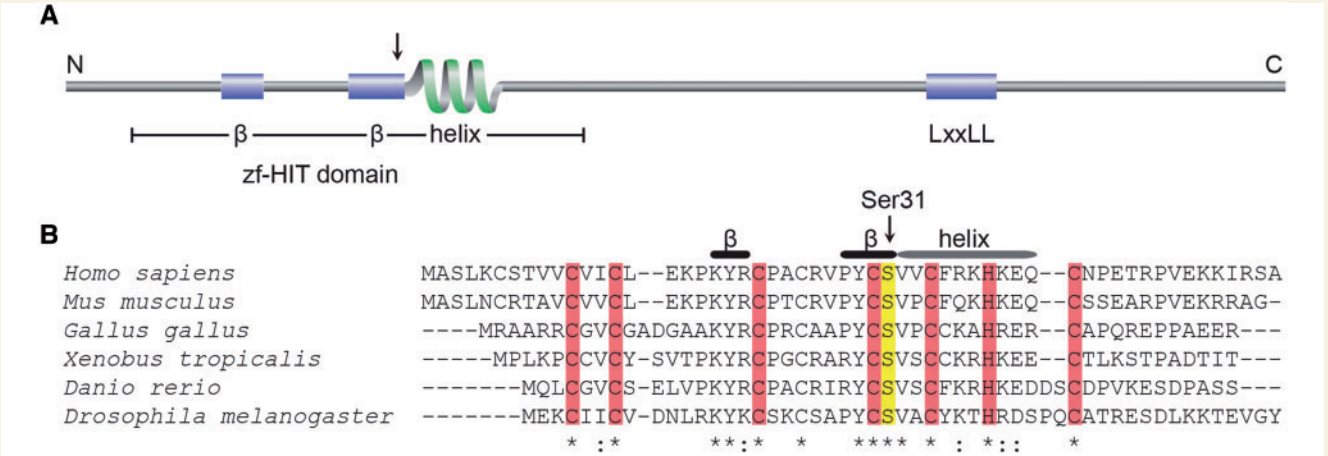

Figure 2 The PEHO mutation affects a highly conserved amino acid in the functional domain of ZNHIT3. (**A**) A schematic picture illustrating the secondary structure of the human ZNHIT3: beta strands, aa 19–21 and 28–31; alpha helix, aa 32–41; LxxLL, aa 101–105. The arrow shows the location of Ser31. (**B**) Multiple alignment of zf-HIT domain of ZNHIT3. Asterisks and colons indicate fully conserved and highly conserved residues, respectively. The residues coordinating zinc atoms are shown with red background and Ser31 with the yellow background.

assay, $P < 0.0001$ for the acetylated-tubulin-visualized cerebellum integrity assay and $P = 0.0003$ for the oedema assay; Fig. 3 and Supplementary Fig. 3). Second, CRISPR-induced deletions in both F0 and F1' 3 dpf zebrafish embryos (generated through an intercross among F0 *znhit3* mutant founders) reproduced consistently the morphant phenotypes in both qualitative and quantitative measures (Fig. 3 and Supplementary Fig. 4).

Testing for rescue of microcephaly, cerebellar integrity and pericardiac oedema showed, consistently, that p.Ser31Leu mutant human mRNA yielded embryos indistinguishable from morphants, suggesting that the p.Ser31Leu represents a loss-of-function allele ($P = 0.72$ from MO and $P < 0.0001$ from MO + wild-type for the optic tectum assay; $P = 0.25$ from MO and $P = 0.0006$ from MO + wild-type for the acetylated-tubulin-visualized cerebellum integrity assay; and $P = 1$ from MO and $P = 0.0001$ from MO + wild-type for the oedema assay; Fig. 3 and Supplementary Fig. 3). Overexpression of either the wild-type or p.Ser31Leu bearing human *ZNHIT3* mRNA did not induce any significant defects (Fig. 3 and Supplementary Fig. 3).

To investigate the cerebellar phenotype we used zebrafish embryos expressing stably NeuroD:GFP, a marker for differentiated granule cells. Both morphants and CRISPR mutants had significant cerebellar defects, with depletion of the neuronal axons across the midline as well as the caudolateral portion of the cerebellum ($P < 0.0001$ for both morphant as well as F0 CRISPR mutant compared to control larvae; Fig. 3 and Supplementary Fig. 5). This aberrant granule cell phenotype could be rescued reproducibly by co-injection of *znhit3*_MO with *ZNHIT3* wild-type ($P < 0.0001$) but not with mutant human mRNA ($P = 0.45$; Supplementary Fig. 5).

Characterization of the ZNHIT3 protein

The effect of the p.Ser31Leu mutation on the putative transcriptional co-regulatory function of ZNHIT3 (Iwahashi *et al.*, 2002; Koppen *et al.*, 2009) was assessed in a series of co-transfection-based reporter gene assays. Under conditions in which TRAP220 (TR-associated protein 220) (Yuan *et al.*, 1998) clearly enhanced the activity of thyroid hormone receptor-dependent transcription, ZNHIT3 enhanced activity only slightly with no further modulatory effect of p.Ser31Leu (Supplementary Fig. 6A and B). In contrast, on HNF4α-dependent transcription (Supplementary Fig. 6C) and in a transcription repression assay ZNHIT3 repressed transcription, and the p.Ser31Leu substitution repressed transcription further (Supplementary Fig. 6D). Using coimmunoprecipitation we showed that the p.Ser31Leu mutation does not compromise the reported interaction (Bizarro *et al.*, 2014; Rothe *et al.*, 2014) of ZNHIT3 with NUFIP1 (Supplementary Fig. 7).

As immunoblotting of the coimmunoprecipitation and reporter gene assay samples repeatedly showed lower protein levels for the p.Ser31Leu variant than wild-type ZNHIT3 (Supplementary Fig. 6C and D), we analysed their stability in intact cells. First, inhibition of protein synthesis with cycloheximide showed that endogenous ZNHIT3 in HeLa cells is short-lived (half-life <2 h) (Fig. 4A). The cycloheximide experiments of COS-1 cells (displaying low endogenous level of ZNHIT3) transfected with ZNHIT3 expression vectors demonstrated that the half-life of the p.Ser31Leu mutant protein was approximately one-fourth of that of wild-type (Fig. 4B). Blocking of the proteasome function by MG132 abolished the difference between wild-type and p.Ser31Leu protein (Fig. 4C), suggesting that the

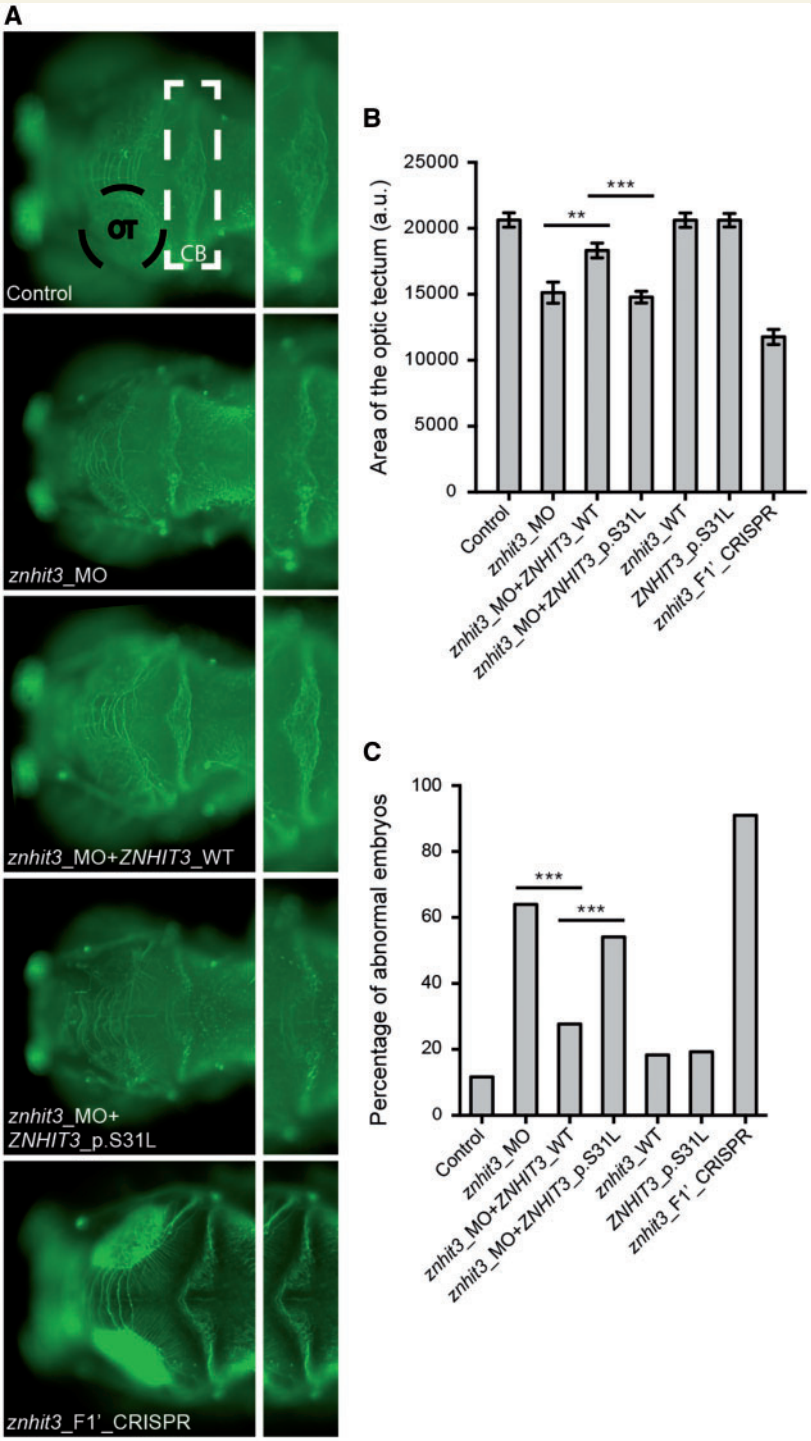

Figure 3 Knockdown and genome editing of *znhit3* in zebrafish causes cerebellar defects and microcephaly. (**A**) Dorsal view of the brains of 3 dpf zebrafish embryos stained with an antibody to acetylated tubulin. Control embryos and embryos injected with a *znhit3* morpholino oligonucleotide (*znhit3*_MO), *znhit3*_MO with *ZNHIT3* wild-type human mRNA (*znhit3*_MO + *ZNHIT3*_WT), *znhit3*_MO with *ZNHIT3* p.Ser31Leu mutant human mRNA (*znhit3*_MO + *ZNHIT3*_p.S31L) and F1' embryos generated through an intercross of F0 *znhit3* CRISPR mutants (*znhit3*_ F1'_CRISPR) are shown. In the control brain, the area of the optic tectum (OT) is highlighted with a black dashed eclipse and the area of the cerebellum (CB) with a white dashed rectangle. Enlarged images of the cerebellum are shown to the right of respective whole brain images. In both the morphant embryos injected with *znhit3*_MO, and the F1' CRISPR mutant embryos there is a reduction of the size of the optic tectum, as well as marked degeneration of the axons forming the midline of the cerebellum, a finding that is consistent with cerebellar atrophy. In the morphant model, both phenotypes were rescued by co-injection of *znhit3*_MO with *ZNHIT3* wild-type human mRNA but not with *ZNHIT3* p.Ser31Leu mutant human mRNA, suggesting that this variant represents a loss-of-function allele. (**B**) Quantification of the optic tectum area in zebrafish larvae at 3 dpf (control $n = 61$, *znhit3*_MO $n = 45$, *znhit3*_MO + *ZNHIT3*_WT $n = 44$, *znhit3*_MO + *ZNHIT3*_p.S31L $n = 42$, *ZNHIT3*_WT $n = 37$, *ZNHIT3*_p.S31L $n = 53$, *znhit3*_F1'_CRISPR $n = 49$). Error bars represent standard error of the mean (SEM). (**C**) Quantification of embryos showing cerebellar defects (control $n = 103$, *znhit3*_MO $n = 86$, *znhit3*_MO + *ZNHIT3*_WT $n = 94$, *znhit3*_MO + *ZNHIT3*_p.S31L $n = 85$, *ZNHIT3*_WT $n = 93$, *ZNHIT3*_p.S31L $n = 109$, *znhit3*_F1'_CRISPR $n = 108$). $^{**}P < 0.01$; $^{***}P < 0.001$. WT = wild-type.

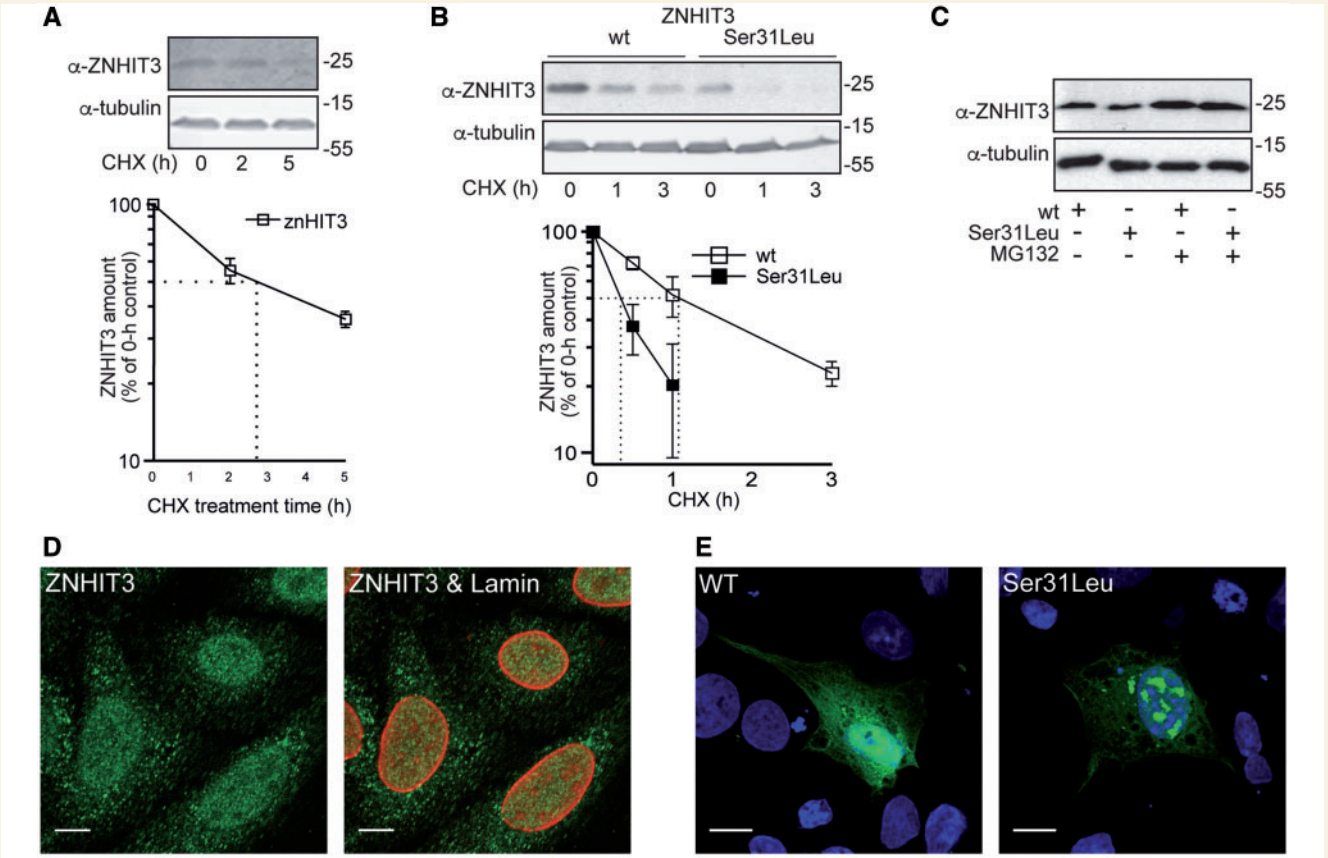

Figure 4 Compromised stability of p.Ser31Leu mutant ZNHIT3. (**A**) HeLa cells were exposed to cycloheximide (CHX), endogenous ZNHIT3 was detected by immunoblotting and its half-life plotted. (**B**) Protein stability measurements in COS-1 cells ectopically expressing wild-type (WT) ZNHIT3 or p.Ser31Leu mutant show that the substitution severely compromises the stability of ZNHIT3. (**C**) Effect of proteasome inhibitor MG132 on ZNHIT3 levels in COS-1 cells. (**D**) Subcellular distribution of endogenous ZNHIT3 (green) in HeLa cells as assessed by immunofluorescence staining and confocal microscopy. An antibody to lamin B1 (red) was used to label nuclear membranes. (**E**) BHK cells transiently transfected with wild-type or p.Ser31Leu ZNHIT3 and treated with cycloheximide for 2.5 h. The cells were stained with an antibody to ZNHIT3 (green) and with Hoechst (blue). Scale bars = 10 μm.

lower steady-state level of the mutant is due to its more rapid proteasomal degradation. Further, both endogenous ZNHIT3 in HeLa cells (Fig. 4D) and wild-type ZNHIT3 in BHK cells (Fig. 4E) displayed punctate staining both in cytosol and nucleus. The p.Ser31Leu mutation did not result in altered subcellular localization of ZNHIT3, but the mutant protein was prone to form large nuclear aggregates (Fig. 4E). Taken together, these data complement the results from zebrafish experiments and suggest that the mechanism for the loss of function is impaired folding of ZNHIT3 rendering it more prone than the wild-type protein to aggregation and degradation.

Neuronal expression of ZNHIT3

As the most striking neuropathology in PEHO syndrome is observed in the cerebellum, characterized by remarkable loss of granule cells and deformed Purkinje cells, and as findings in zebrafish embryos indicated granule cell defects, we analysed the ZNHIT3 protein expression in mouse cerebellum. The expression of ZNHIT3 was evident in proliferating foetal granule cell precursors at embryonic Day 16.5, in proliferating and post-mitotic granule cells at postnatal Days 3 and 10 (Fig. 5A) and was still visible, though less prominent, in mature postnatal Day 21 cerebellum (Fig. 5B). However, expression of ZNHIT3 in cerebellar Purkinje cells was strong at postnatal Days 10 and 21. Expression analysis of ZNHIT3 in Bergmann glia, which is important for the migration of the cerebellar granule cells (Rakic, 1971), remained inconclusive, since co-localization of ZNHIT3 with the glial marker GFAP was only partial (Fig. 5B and inset). In cultured postnatal cerebellar granule cells the expression of ZNHIT3 was strong and mainly nuclear (Fig. 5C), consistent with findings in cell lines.

Knockdown of *Znhit3* by RNAi in cerebellar granule cells

To investigate the impact of ZNHIT3 deficiency on cerebellar pathology, we first used a plasmid-based method of RNAi to

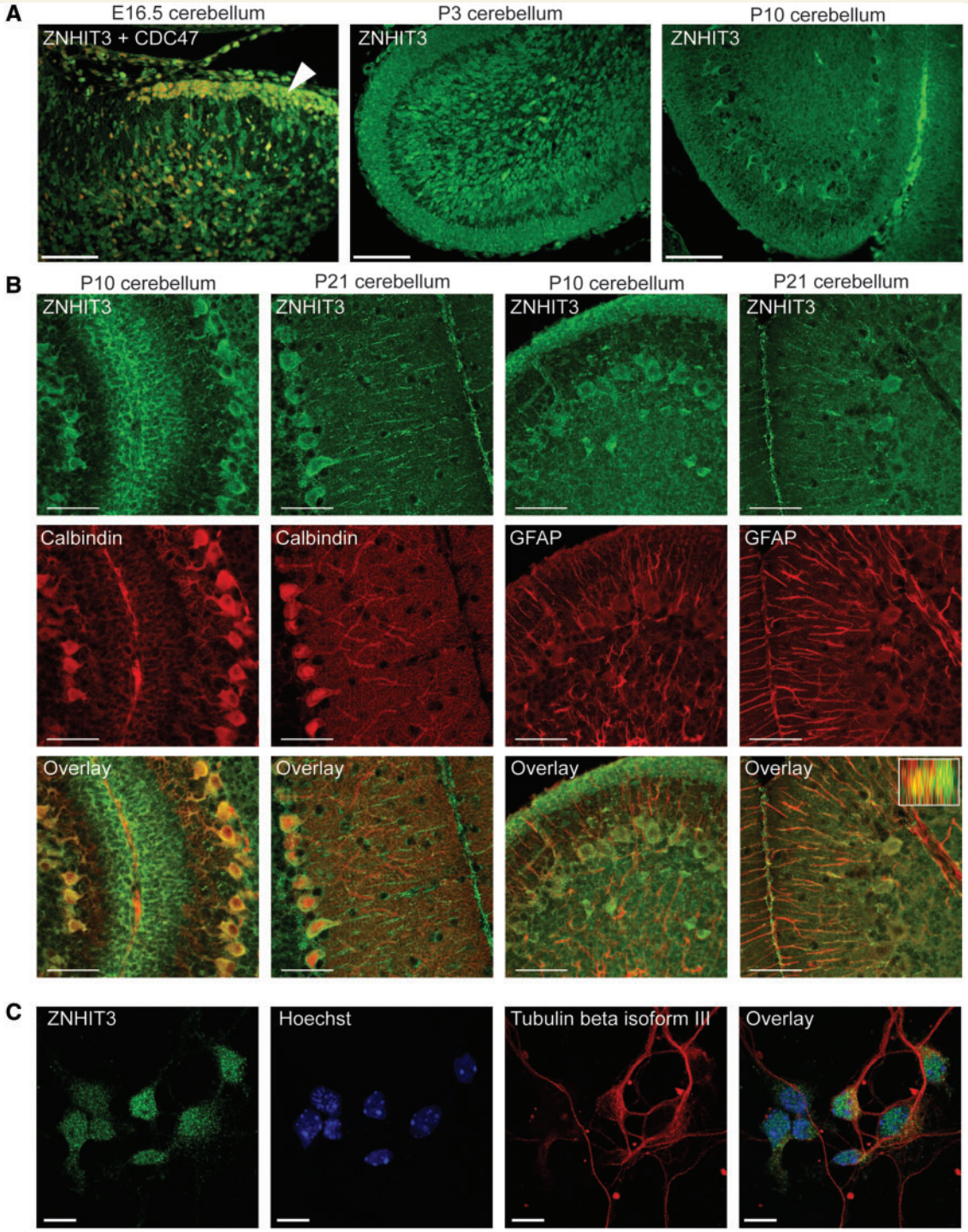

Figure 5 Endogenous ZNHIT3 expression in the developing mouse cerebellum and cultured cerebellar granule cells. (**A**) Developing cerebellar cortex at embryonic Day (E)16.5, postnatal Day (P)3 and P10 were stained with an antibody to ZNHIT3 (green). The section at E16.5 was also stained with an antibody to CDC47 (red), a marker for mitotic cells. An arrowhead shows foetal precursor cells at E16.5. Pictures were captured with an epifluorescence microscope. Scale bars = 50 μm. (**B**) Mouse cerebellar cortex at P10 and P21 stained with an antibody to ZNHIT3 (green) and to calbindin or GFAP (red), markers for Purkinje and astroglial cells, respectively. Pictures are average projections of stacks of four consecutive confocal microscope images. An insert shows a reconstructed orthogonal projection of the stack. Scale bars = 50 μm. (**C**) Endogenous ZNHIT3 expression in cultured P5 mouse cerebellar granule cells. The cells were stained with antibodies to ZNHIT3 (green) and tubulin, beta III isoform (red), a marker for neurons, and with Hoechst (blue). Scale bars = 20 μm.

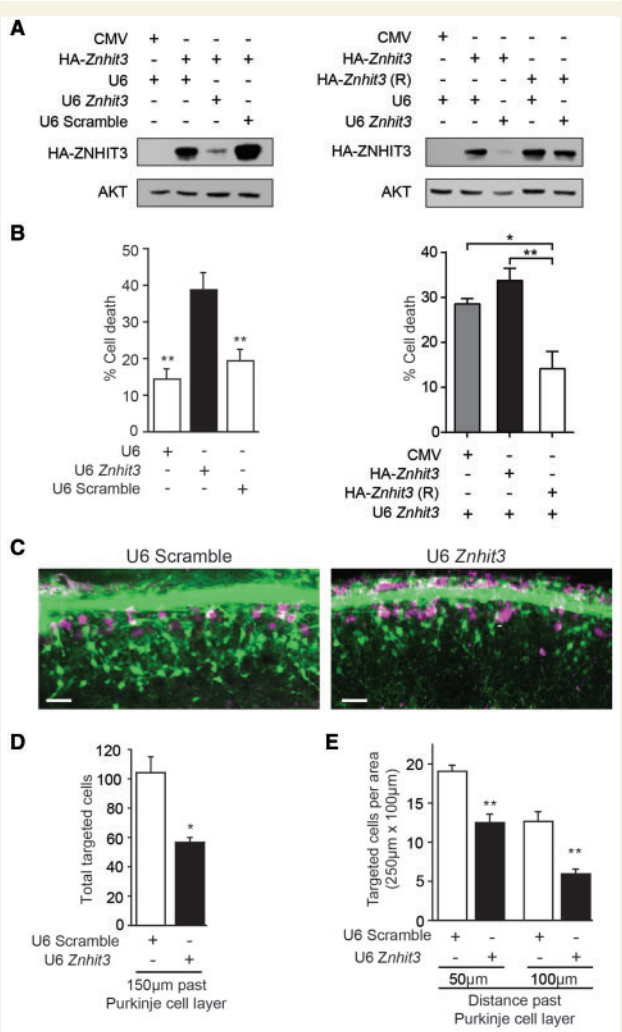

Figure 6 ZNHIT3 deficiency leads to death and impaired migration of mouse cerebellar granule neurons. (**A**) *Left*: Lysates of 293T cells transfected with an expression vector encoding haemagglutinin (HA) -tagged mouse ZNHIT3 (HA-*Znhit3*) or control CMV plasmid together with the *Znhit3* hpRNA (U6 *Znhit3*), control U6, or U6 Scramble plasmids, immunoblotted with the antibodies to HA and AKT. *Right*: Lysates of 293T cells transfected with mouse HA-*Znhit3*, Rescue HA-*Znhit3* (R), or control CMV plasmid together with the *Znhit3* hpRNA or control U6 plasmid, immunoblotted (as in *left*). (**B**) *Left*: Percentage of cell death of GFP-positive mouse cerebellar granule neurons transfected with the *Znhit3* hpRNA, control U6, or control Scramble plasmids together with the GFP expression plasmid after 72 h in culture, represented as mean ± SEM (U6 control plasmid: 14.3 ± 2.8; *Znhit3* hpRNA: 38.7 ± 4.7; Scramble: 19.4 ± 3.1; $^{**}P < 0.01$; $n = 3$). *Right*: Neuronal death (as in *left*) of cells transfected with the *Znhit3* hpRNA and wild-type HA-*Znhit3*, Rescue HA-*Znhit3* (R), or control CMV plasmids (HA-*Znhit3* + *Znhit3* hpRNA: 33.737 ± 2.697; Rescue HA-*Znhit3* (R) + *Znhit3* hpRNA: 14.15 ± 3.282; CMV + *Znhit3* hpRNA: 28.553 ± 1.86; $^{*}P < 0.05$; $^{**}P < 0.01$; $n = 3$). (**C**) *Ex vivo* cerebellar slice cultures injected with control Scramble or *Znhit3* hpRNA and stained with antibodies to GFP (green) and calbindin (magenta) showing fewer numbers of GFP-positive targeted cells located past the calbindin-positive stained Purkinje cell layer in *Znhit3* injected compared to Scramble control. Scale bar = 40 μm. (**D**) Quantification of GFP-positive targeted cells shown in **C** located 150 μm past Purkinje cell layer (*Znhit3* hpRNA: 57.0 ± 3.0, Scramble: 104.3 ± 10.3; Mann-Whitney; $^{*}P < 0.05$; $n = 3$). (**E**) Quantification of GFP-positive targeted cell location shown in **C**. Cell counts per fixed area (250 μm × 100 μm) are shown at 50 μm (*Znhit3* hpRNA: 12.6 ± 1.0, Scramble: 19 ± 0.85) and at 100 μm (*Znhit3* hpRNA: 5.9 ± 0.7, Scramble: 12.7 ± 1.2; Mann-Whitney; $^{**}P < 0.01$; $n = 3$) past the calbindin-positive staining Purkinje cell layer.

reduce the expression of mouse *Znhit3* in 293T cells (Fig. 6A) and in cultured primary mouse cerebellar granule neurons (Fig. 6B). Knockdown of *Znhit3* sensitized the neurons to death, and the specificity of the effect was demonstrated by co-expressing a 'rescue' form of *Znhit3* (Zn-HIT3R) resistant to Znhit3 RNAi (Fig. 6A and B). Further, knocking down *Znhit3* expression *ex vivo* in cerebella harvested from postnatal Day 8 mouse pups resulted in reduced numbers of ZNHIT3-deficient cerebellar granule neurons located at increased distances away from the external granule cell layer (Fig. 6C). Reduced numbers of neurons were found within 50 μm, 100 μm, and 150 μm of the calbindin-positive Purkinje cell layer compared to control (Fig. 6D and E). These data are consistent with our observation of ectopic granule neurons in cerebella of PEHO syndrome patients (Fig. 1H). Taken together, these data show that compromised neuronal survival and impaired migration contribute to the cerebellar pathology associated with defective ZNHIT3 function.

Discussion

Here we describe that loss-of-function of ZNHIT3, caused by homozygosity for the p.Ser31Leu variant, underlies autosomal recessive PEHO syndrome. The observed carrier frequency (~1%) of p.Ser31Leu in the Finnish population is in line with the estimated incidence of PEHO syndrome (Somer, 1993*a*). Definition of the clinical characteristics in a molecularly uniform patient cohort (Table 1) confirmed the validity of the previously established clinical criteria (Somer, 1993*a*) with the exception of infantile spasms and hypsarrhythmia, which are not present in all PEHO patients. We thus suggest that infantile spasms may be removed as an essential clinical criterion for PEHO syndrome. The patients presented uniform neuroradiological findings with progressive cerebellar atrophy and dysmyelination as essential diagnostic criteria. The clinical presentation among affected siblings was very similar.

Recently, five other genes have been implicated in patients with PEHO-like features (Gawlinski *et al.*, 2016; Langlois *et al.*, 2016; Nahorski *et al.*, 2016). A homozygous frame-shift deletion in *CCDC88A*, which encodes an actin binding protein, with an essential role in cellular migration and early development of mouse brain, was reported in three consanguineous individuals (Nahorski *et al.*, 2016). However, the presence of microcephaly at birth as well as polymicrogyria and pachygyria on MRI

Table 1 Occurrence of clinical features in PEHO patients with the p.Ser31Leu mutation in *ZNHIT3*

Main feature	More detailed description	*n*/*n*[a]	Percentage
Hypotonia	Infantile, usually neonatal	26/26	100
Convulsive disorder		27/27	100
	Infantile spasms with hypsarrhythmia	24/27	89
	Age of onset, infantile spasms: 2–10 months	22/24	
	Initial seizure type other than infantile spasms	4/27	15
Profound motor and intellectual disability		27/27	100
	Complete absence of speech	25/27	93
Absence or early loss of visual fixation		27/27	100
	Atrophy of optic discs	19/24	79
	ERG normal	18/18	100
	VEP abnormal	18/21	86
Progressive[b] brain atrophy		24/24	100
	Predominantly cerebellum and brain stem	24/24	100
	Dysmyelination on MRI	16/16	100
Oedema	Limbs	21/28	75
Typical dysmorphic features		23/24	96
Brisk tendon reflexes	At early stage; later, no reflexes	25/27	93

[a]Includes three patients without confirmed mutation status in the patient sample, but detected heterozygous carrier status for p.Ser31Leu in parent samples.
[b]Progressive in patients with multiple CT/MRI scans.

argue against the diagnosis of PEHO syndrome in these patients. A dominant *de novo* missense variant in the motor domain of the KIF1A motor protein, involved in the anterograde transport of synaptic-vesicle precursors along axons (Riviere *et al.*, 2011), was reported in one patient (Langlois *et al.*, 2016). Based on the MRI figure in the paper, myelination in this patient seemed to be less severely compromised than is typical for Finnish patients with PEHO syndrome, suggesting that the patient does not have PEHO syndrome. Indeed, in our cohort of Finnish PEHO-like patients we have identified one patient with a *de novo KIF1A* mutation (Lehesjoki, personal communication). Finally, identification of *de novo* mutations both in *GNAO1* and in *HESX1*, and in *CDKL5* in patients with PEHO-like phenotypes led to the suggestion that PEHO syndrome may represent a severe end of the spectrum of the early-onset encephalopathies (Gawlinski *et al.*, 2016).

Loss of *znhit3* in zebrafish caused defective cerebellar development, which manifested as aberrant granule cells and misaligned parallel fibres in the cerebellar midline and caudolateral cerebellar portion. These findings further highlight the granule cells as the cerebellar cell type predominantly affected in ZNHIT3 deficiency. Since the first neuropathological evaluation of PEHO patients (Haltia and Somer, 1993), it has been speculated that the almost total loss of inner granule cell layer could be due to granule cell death prior to or during migration (Somer, 1993*b*). Similar defects in the migration and survival of granule cells were further recapitulated through preliminary experiments in the mouse and zebrafish we report herein. To which extent increased granule cell death and impaired migration contribute to the phenotype remains to be explored through additional *in vivo* studies. Towards this, the generation of a stable mutant *znhit3* line is necessary in order to study the specific disease pathomechanisms, as transient knockdown systems and mosaic F0 animals are likely to display weaker phenotypes compared to null models, as exemplified by the phenotypic severity of the F1' animals compared to the milder effects of the MO and the CRISPR editing. Nevertheless, the fact that all three organisms, human, mouse and zebrafish, display similar cellular and organismal defects at different evolutionary stages, suggests a critical and conserved molecular function for ZNHIT3 in cerebellum and establishes compromised ZNHIT3 function as the causative determinant in PEHO pathology.

ZNHIT3 (previously called TRIP3, TR interacting protein 3) was first reported to interact with rat TR beta (TRβ1) in the presence of thyroid hormone (Lee *et al.*, 1995) and with retinoid X receptor (RXR) in a 9-*cis*-retinoic acid-responsive manner (Lee *et al.*, 1995). However, the functional consequences of these interactions were not tested. Later, ZNHIT3 was reported to co-regulate the activity of hepatocyte nuclear factor 4-alpha (HNF4α) (Iwahashi *et al.*, 2002) and that of peroxisome proliferator-activated receptor gamma (PPARγ) (Koppen *et al.*, 2009). Even though our *in vitro* reporter gene assays did not confirm the suggested transcriptional co-regulatory function of ZNHIT3, it is possible that the effects of mutated ZNHIT3 would be, at least in part, mediated through perturbation in transcriptional regulation during periods critical for cerebellar development. It is interesting to note the similarity of the cerebellar changes between PEHO syndrome patients (Haltia and Somer, 1993) and thyroid hormone deficient or thyroid hormone receptor gene targeted rodents (Yuan *et al.*, 1998; Hashimoto

et al., 2001; Horn and Heuer, 2010; Portella et al., 2010; Fauquier et al., 2011). A dominant-negative mutation in the gene encoding the TRα1 receptor has been shown to primarily alter the differentiation of Purkinje cells and Bergman glia leading to secondary impairment of migration and terminal differentiation of granule cell precursors (Fauquier et al., 2014). Our data on ZNHIT3 being expressed not only in Purkinje cells, but also in proliferating and mature granule neurons imply that ZNHIT3 has specific functions also in granule neurons. Recent reports linking ZNHIT3 to small nucleolar ribonucleoprotein particle assembly and thus possibly to pre-ribosomal RNA processing via its interaction with nuclear fragile X mental retardation protein interacting protein 1 (NUFIP1) (Bardoni et al., 2003; Rothe et al., 2014) imply that ZNHIT3 may have roles beyond transcriptional regulation. However, while we were able to confirm the interaction of ZNHIT3 with NUFIP1, the p.Ser31Leu substitution did not influence this interaction.

The establishment of the nuclear functions of ZNHIT3 will be a next important step in understanding the pathomechanism of PEHO syndrome with focus on periods critical for proliferation, migration and maturation of cerebellar granule cells. It will also be intriguing to ask whether some of the genes known to phenocopy aspects of the core PEHO pathology, might also be either regulated by ZNHIT3 or partake in similar signalling cascades. At present, ZNHIT3 is the only nuclear factor implicated in this disorder. Identification of the remaining PEHO-like causing proteins and determining whether some/all of these proteins are involved in the same core mechanisms as ZNHIT3 thus has the possibility, not only to inform the molecular aetiology of a broader group of disorders but also to unravel key mechanisms required for normal cerebellar and cerebral development.

Acknowledgements

We thank the patients and their families for their contribution to this study and clinicians for sending patient samples to this study. H. Hellgren, A. Malesz, and M. Räsänen are thanked for technical assistance, and E. Govek for advice on cerebellar electroporations. M. Haltia is thanked for his invaluable advice. Genome-wide SNP genotyping, next generation sequencing and variant calling were performed at the Institute for Molecular Medicine Finland (FIMM) Technology Centre, University of Helsinki. The authors would like to thank the Exome Aggregation Consortium and the groups that provided exome variant data for comparison. A full list of contributing groups can be found at http://exac.broadinstitute.org/about.

Funding

This project was funded by Folkhälsan Research Foundation (to A.-E.L.), Sloan Research Fellowship (to M.K.L.), Arvo and Lea Ylppö Foundation (to A.-K.A.), Doctoral Programme in Biomedicine University of Helsinki (to M.M.), Emil Aaltonen Foundation (to A.-K.A.), Foundation for Pediatric Research, Ulla Hjelt fund (to J.H.), and Helsinki University Central Hospital Research Fund (to A.-K.A. and J.H.). M.K.L. is a NYSCF – Robertson Investigator. J.J.P. laboratory is supported by the Academy of Finland and the Sigrid Jusélius Foundation.

Supplementary material

Supplementary material is available a *Brain* online.

References

Alfadhel M, Yong SL, Lillquist Y, Langlois S. Precocious puberty in two girls with PEHO syndrome: a clinical feature not previously described. J Child Neurol 2011; 26: 851–7.

Anttonen AK, Hilander T, Linnankivi T, Isohanni P, French RL, Liu Y, et al. Selenoprotein biosynthesis defect causes progressive encephalopathy with elevated lactate. Neurology 2015; 85: 306–15.

Bardoni B, Willemsen R, Weiler IJ, Schenck A, Severijnen LA, Hindelang C, et al. NUFIP1 (nuclear FMRP interacting protein 1) is a nucleocytoplasmic shuttling protein associated with active synaptoneurosomes. Exp Cell Res 2003; 289: 95–107.

Bizarro J, Charron C, Boulon S, Westman B, Pradet-Balade B, Vandermoere F, et al. Proteomic and 3D structure analyses highlight the C/D box snoRNP assembly mechanism and its control. J Cell Biol 2014; 207: 463–80.

Borck G, Hog F, Dentici ML, Tan PL, Sowada N, Medeira A, et al. BRF1 mutations alter RNA polymerase III-dependent transcription and cause neurodevelopmental anomalies. Genome Res 2015; 25: 155–66.

Caraballo RH, Pozo AN, Gomez M, Semprino M. PEHO syndrome: a study of five Argentinian patients. Pediatr Neurol 2011; 44: 259–64.

Chitty LS, Robb S, Berry C, Silver D, Baraitser M. PEHO or PEHO-like syndrome? Clin Dysmorphol 1996; 5: 143–52.

Christensen R, de la Torre-Ubieta L, Bonni A, Colon-Ramos DA. A conserved PTEN/FOXO pathway regulates neuronal morphology during C. elegans development. Development 2011; 138: 5257–67.

Cuadrado A, Corrado N, Perdiguero E, Lafarga V, Munoz-Canoves P, Nebreda AR. Essential role of p18Hamlet/SRCAP-mediated histone H2A.Z chromatin incorporation in muscle differentiation. EMBO J 2010; 29: 2014–25.

Drerup CM, Nechiporuk AV. JNK-interacting protein 3 mediates the retrograde transport of activated c-Jun N-terminal kinase and lysosomes. PLoS Genet 2013; 9: e1003303.

Fauquier T, Chatonnet F, Picou F, Richard S, Fossat N, Aguilera N, et al. Purkinje cells and Bergmann glia are primary targets of the TRalpha1 thyroid hormone receptor during mouse cerebellum postnatal development. Development 2014; 141: 166–75.

Fauquier T, Romero E, Picou F, Chatonnet F, Nguyen XN, Quignodon L, et al. Severe impairment of cerebellum development in mice expressing a dominant-negative mutation inactivating thyroid hormone receptor alpha1 isoform. Dev Biol 2011; 356: 350–8.

Field MJ, Grattan-Smith P, Piper SM, Thompson EM, Haan EA, Edwards M, et al. PEHO and PEHO-like syndromes: report of five Australian cases. Am J Med Genet A 2003; 122A: 6–12.

Gaudilliere B, Shi Y, Bonni A. RNA interference reveals a requirement for myocyte enhancer factor 2A in activity-dependent neuronal survival. J Biol Chem 2002; 277: 46442–6.

Gawlinski P, Posmyk R, Gambin T, Sielicka D, Chorazy M, Nowakowska B, et al. PEHO syndrome may represent phenotypic

expansion at the severe end of the early-onset encephalopathies. Pediatr Neurol 2016; 60: 83–7.
Giulian D, Baker TJ. Characterization of ameboid microglia isolated from developing mammalian brain. J Neurosci 1986; 6: 2163–78.
Haltia M, Somer M. Infantile cerebello-optic atrophy. Neuropathology of the progressive encephalopathy syndrome with edema, hypsarrhythmia and optic atrophy (the PEHO syndrome). Acta Neuropathol 1993; 85: 241–7.
Hashimoto K, Curty FH, Borges PP, Lee CE, Abel ED, Elmquist JK, et al. An unliganded thyroid hormone receptor causes severe neurological dysfunction. Proc Natl Acad Sci USA 2001; 98: 3998–4003.
He F, Umehara T, Tsuda K, Inoue M, Kigawa T, Matsuda T, et al. Solution structure of the zinc finger HIT domain in protein FON. Protein Sci 2007; 16: 1577–87.
Heery DM, Kalkhoven E, Hoare S, Parker MG. A signature motif in transcriptional co-activators mediates binding to nuclear receptors. Nature 1997; 387: 733–6.
Horn S, Heuer H. Thyroid hormone action during brain development: more questions than answers. Mol Cell Endocrinol 2010; 315: 19–26.
Iwahashi H, Yamagata K, Yoshiuchi I, Terasaki J, Yang Q, Fukui K, et al. Thyroid hormone receptor interacting protein 3 (trip3) is a novel coactivator of hepatocyte nuclear factor-4alpha. Diabetes 2002; 51: 910–4.
Jao LE, Wente SR, Chen W. Efficient multiplex biallelic zebrafish genome editing using a CRISPR nuclease system. Proc Natl Acad Sci USA 2013; 110: 13904–9.
Koppen A, Houtman R, Pijnenburg D, Jeninga EH, Ruijtenbeek R, Kalkhoven E. Nuclear receptor-coregulator interaction profiling identifies TRIP3 as a novel peroxisome proliferator-activated receptor gamma cofactor. Mol Cell Proteomics 2009; 8: 2212–26.
Langlois S, Tarailo-Graovac M, Sayson B, Drogemoller B, Swenerton A, Ross CJ, et al. De novo dominant variants affecting the motor domain of KIF1A are a cause of PEHO syndrome. Eur J Hum Genet 2016; 24: 949–53.
Lee JW, Choi HS, Gyuris J, Brent R, Moore DD. Two classes of proteins dependent on either the presence or absence of thyroid hormone for interaction with the thyroid hormone receptor. Mol Endocrinol 1995; 9: 243–54.
Lehtinen MK, Tegelberg S, Schipper H, Su H, Zukor H, Manninen O, et al. Cystatin B deficiency sensitizes neurons to oxidative stress in progressive myoclonus epilepsy, EPM1. J Neurosci 2009; 29: 5910–5.
Lehtinen MK, Yuan Z, Boag PR, Yang Y, Villen J, Becker EB, et al. A conserved MST-FOXO signaling pathway mediates oxidative-stress responses and extends life span. Cell 2006; 125: 987–1001.
Longman C, Tolmie J, McWilliam R, MacLennan A. Cranial magnetic resonance imaging mistakenly suggests prenatal ischaemia in PEHO-like syndrome. Clin Dysmorphol 2003; 12: 133–6.
Nahorski MS, Asai M, Wakeling E, Parker A, Asai N, Canham N, et al. CCDC88A mutations cause PEHO-like syndrome in humans and mouse. Brain 2016; 139 (Pt 4): 1036–44.
Portella AC, Carvalho F, Faustino L, Wondisford FE, Ortiga-Carvalho TM, Gomes FC. Thyroid hormone receptor beta mutation causes severe impairment of cerebellar development. Mol Cell Neurosci 2010; 44: 68–77.
Purcell S, Neale B, Todd-Brown K, Thomas L, Ferreira MA, Bender D, et al. PLINK: a tool set for whole-genome association and population-based linkage analyses. Am J Hum Genet 2007; 81: 559–75.
Rakic P. Neuron-glia relationship during granule cell migration in developing cerebellar cortex. A Golgi and electronmicroscopic study in Macacus Rhesus. J Comp Neurol 1971; 141: 283–312.
Riviere JB, Ramalingam S, Lavastre V, Shekarabi M, Holbert S, Lafontaine J, et al. KIF1A, an axonal transporter of synaptic vesicles, is mutated in hereditary sensory and autonomic neuropathy type 2. Am J Hum Genet 2011; 89: 219–30.
Rothe B, Saliou JM, Quinternet M, Back R, Tiotiu D, Jacquemin C, et al. Protein Hit1, a novel box C/D snoRNP assembly factor, controls cellular concentration of the scaffolding protein Rsa1 by direct interaction. Nucleic Acids Res 2014; 42: 10731–47.
Salonen R, Somer M, Haltia M, Lorentz M, Norio R. Progressive encephalopathy with edema, hypsarrhythmia, and optic atrophy (PEHO syndrome). Clin Genet 1991; 39: 287–93.
Schulte EC, Kousi M, Tan PL, Tilch E, Knauf F, Lichtner P, et al. Targeted resequencing and systematic in vivo functional testing identifies rare variants in MEIS1 as significant contributors to restless legs syndrome. Am J Hum Genet 2014; 95: 85–95.
Somer M. Diagnostic criteria and genetics of the PEHO syndrome. J Med Genet 1993a; 30: 932–6.
Somer M. The PEHO syndrome. Helsinki: University of Helsinki; 1993b.
Somer M, Sainio K. Epilepsy and the electroencephalogram in progressive encephalopathy with edema, hypsarrhythmia, and optic atrophy (the PEHO syndrome). Epilepsia 1993; 34: 727–31.
Somer M, Salonen O, Pihko H, Norio R. PEHO syndrome (progressive encephalopathy with edema, hypsarrhythmia, and optic atrophy): neuroradiologic findings. AJNR Am J Neuroradiol 1993a; 14: 861–7.
Somer M, Setälä K, Kivelä T, Haltia M, Norio R. The PEHO syndrome (progressive encephalopathy with oedema, hypsarrhythmia and optic atrophy) Ophthalmological findings and differential diagnosis. Neuro Ophthalmol 1993b; 13: 65–74.
Walker SD, Kälviäinen R. Non-vision adverse events with vigabatrin therapy. Acta neurologica Scandinavica Supplementum 2011: 72–82.
Yang YJ, Baltus AE, Mathew RS, Murphy EA, Evrony GD, Gonzalez DM, et al. Microcephaly gene links trithorax and REST/NRSF to control neural stem cell proliferation and differentiation. Cell 2012; 151: 1097–112.
Yuan CX, Ito M, Fondell JD, Fu ZY, Roeder RG. The TRAP220 component of a thyroid hormone receptor- associated protein (TRAP) coactivator complex interacts directly with nuclear receptors in a ligand-dependent fashion. Proc Natl Acad Sci USA 1998; 95: 7939–44.